JOURNAL OF SPACECRAFT AND ROCKETS
Vol. 37, No. 2, March–April 2000

Validation of the Enhanced URANUS Nonequilibrium Navier–Stokes Code

H.-H. Frühauf,* M. Fertig,† and S. Kanne‡
University of Stuttgart, D-70550 Stuttgart, Germany

The enhancements that have recently been implemented into the URANUS nonequilibrium Navier–Stokes code in order to further improve the gas-phase modeling and the gas-surface interaction modeling are summarized. Validation of the improved code was performed against various free-flight experiments such as BSUV II, MIRKA, FIRE II, Stardust, the air nozzle flow experiment of Sharma/Gilmore, and the DLR body-flap experiment. The flight experiments have been partially recomputed to demonstrate the influence of the enhancements. The influence of the enhanced modeling on postshock, boundary layer and wake flow and aerothermal loads are discussed in detail for low to high reentry velocities. To demonstrate the improved modeling and credibility of the enhanced code, measured aerothermal loads were recomputed along the flight trajectories for a wide gas state and velocity range.

Introduction

THE objective of this article is to summarize the enhancements recently implemented into the URANUS code and to report new validation results. Many literature sources are provided that describe the theory of the enhancements in detail.

The enhanced URANUS code takes into account all internal degrees of freedom in the gas-phase modeling. Capitelli's newly determined collision integrals and the more accurate mixing rule of Chapman–Cowling have been implemented in the updated transport coefficient model. Locally and spectrally resolved plasma radiation can be computed uncoupled and coupled to predict optical measurements or radiation cooling in high-velocity flows.

For a comprehensive validation of the enhanced URANUS code, nonequilibrium flows with different thermophysical processes were studied for a large density and velocity range. First the thermochemical relaxation model was validated for an air nozzle flow experiment at moderate temperatures. Then well-known high-speed free-flight experiments of ballistic capsules were recomputed to investigate the influence of electronic excitation and enhanced transport coefficient modeling on these partially ionized flows. The predictability of pressure and partial catalytic heat flux along the forebody of the MIRKA capsule with a C/SiC-TPS surface along the trajectory was investigated in some detail. In all capsule experiments measurements were performed along the convex-shaped forebody under laminar flow conditions. Hence, the free-flight validations are primarily performed for these laminar nonequilibrium forebody flows, which include postshock, stagnation-point, and expansion flows. Finally a laminar separated, high-enthalpy, hot-surface body-flap experiment is reconstructed to validate the enhanced URANUS code for a more complex nonequilibrium flow.

Computational Technique

The Navier–Stokes code URANUS was developed for the accurate simulation of nonequilibrium flows around reentry vehicles over a wide altitude-velocity range.[1] The unsteady, compressible Navier–Stokes equations in integral form were discretized in space using the cell-centered finite volume approach on structured grids. Inviscid fluxes were calculated with Roe's approximative Riemann solver, and second-order accuracy is achieved using the MUSCL concept. Time integration was accomplished by the Euler backward scheme, and the resulting implicit system of equations was solved iteratively by Newton's method. Although the source term Jacobians were implemented exactly, the Jacobians of the inviscid flux terms were only computed approximately following Barth. The viscous Jacobians were obtained from the thin-layer approximation of the viscous fluxes. The resulting linear system of equations was solved iteratively by Jacobi line relaxation, and an underlying subiteration scheme was used to minimize the inversion error. The boundary conditions were implemented implicitely to preserve the high convergence rate of the Newton-like method. Slip and no-slip surface conditions are available, and different models for surface catalysis were implemented.

The nonequilibrium boundary layers were highly resolved and as small as the mean free-path scale at the surface. Courant–Friedrichs–Lewy numbers up to 1000 were obtained in nonequilibrium computations. A sufficient convergence grade, which is important for an accurate prediction of surface heat flux, was obtained with the Newton-like method. The program was parallelized by domain decomposition. To ensure portability, the MPI message-passing paradigm was used. The parallel code maintains the sequential code's convergence, and a nearly linear scale-up was demonstated for up to 512 processors on Cray T3E.

Enhanced Modeling

Thermochemical Relaxations

The coupled-vibration-chemistry-vibration (CVCV) gas-phase model[2] was recently extended to include the influence of rotational excitation of the molecules.[3] Starting from state-selective rates, multitemperature rates depending on the translational temperature as well as on vibrational and rotational temperatures were obtained by averaging over the distribution function of internal energies. The model can be used for all types of reactions that are important in high-enthalpy flows (e.g., dissociation, exchange, and associative ionization reactions). Consistent with the modeling of the production rates, the production rates of vibrational and rotational energies caused by chemical reactions were computed. Using quasi-classical trajectory calculations, the parameters of the CVCV model were newly calibrated for dissociation and exchange reactions.[4] With these improvements nonequilibrium flows experience more dissociation because the dissociation energy is lowered by the rotational excitation. The kinetics of the Zeldovich reactions are now in accordance with quasi-classical trajectory theory. The improved NO-chemistry modeling in the URANUS code was validated indirectly by means of a spectrometer simulation performed with the PARADE radiation code[5] and the HERTA radiation transport code[6] for the Bow Shock Ultraviolet Experiment II, where spectra in the wavelength range of NO have been measured.[7] With the exception of high altitudes where weak radiation signals do occur, good agreement was

Presented as Paper 99-3683 at the 33rd AIAA Thermophysics Conference, Norfolk, VA, 28 June–1 July 1999; received 22 July 1999; revision received 11 November 1999; accepted for publication 9 December 1999.

*Senior Scientist, Institut für Raumfahrtsysteme, Pfaffenwaldring 31. Member AIAA.
†Research Scientist, Institut für Raumfahrtsysteme, Pfaffenwaldring 31.
‡Research Scientist, Institut für Raumfahrtsysteme, Pfaffenwaldring 31. Member AIAA.

obtained between measured and simulated spectra along the trajectory. Furthermore, the vibration-vibration (V-V) energy-exchange model has been extended for low translational temperatures, which occur in the vicinity of cold surfaces and in wakes.[8] Here the significant decrease of the V-V transition probability with decreasing translational temperature has been modeled according to Rapp.[9] It is validated against Sharma/Gilmore's air nozzle flow experiment.

Electronic Excitation

Up to now, electronic excitation has not been considered in the URANUS code. For significantly ionized flows the influence of electronic excitation on the ion chemistry of atoms was modeled via the quasi-steady-state (QSS) theory of Park.[10] The theory uses the fact that population density change of an energy level occurs much slower than the involved collision processes. The QSS theory has been consistently implemented in the multitemperature Navier–Stokes code, which assumes Boltzmann distributions for the other energies.[8] According to CVCV-model principles, the influence of electronic excitation on the ionization rate of atomic nitrogen and oxygen is modeled by nonequilibrium factors. The influence of electronic excitation on the postshock ionization of atomic nitrogen and oxygen was investigated for the FIRE II experiment.

Transport Coefficients

In dissociated and ionized reentry flows strong gradients are observed in density, temperatures, and velocities. To describe the exchange of mass, momentum, and energy under these conditions, Chapman–Cowling's first approximations for the transport coefficients, translational thermal conductivity of heavy particles, viscosity, and mass diffusion were implemented into the URANUS Code, as well as the second approximation of thermal conductivity of electrons.[11] Results of the new model were compared with the simplified model of Gupta and Yos for the Stardust capsule flow. Furthermore, Capitelli's newly computed collision integrals have been implemented into the URANUS and, code results were presented by Fertig et al.[11]

Gas-Surface Interaction Modeling

The finite rate catalytic behavior of a thermal protection system (TPS) surface influences the surface heat flux significantly. Kinetic gas-surface interaction models were incorporated in the URANUS code in order to take into account near-surface rarefaction effects in leeward flows, base flows, and general reentry flows at high altitudes. A detailed catalysis model for SiO_2-surfaces has been implemented by Daiss[12] into the URANUS code, which distinguishes adsorption, desorption, and recombination reactions according to the Eley–Rideal and Langmuir–Hinshelwood mechanisms, as well as dissociative adsorption reactions. Furthermore, an expression for the estimation of the chemical energy accommodation coefficient of the Eley–Rideal mechanism has been derived. This detailed model, which consists of elementary reactions, is able to describe the non-Arrhenius behavior of the recombination coefficients and has been successfully validated for the shuttle reentry, from the slip-flow range close to the perfect-gas range.

Finite rate catalytic behavior can also be predicted by a purely phenomenological or simplified global model, which attempts to match newly available experimental data obtained in high-enthalpy facilities for a large surface temperature range by a temperature-dependent expression for the overall recombination coefficients of the atomic species. In this simple single-step model the chemical energy accommodation coefficient is assumed to be unity. We have shown in the case of the shuttle windward flow that detailed and global catalysis models nearly predict the same surface heat flux. Because SiO_2-coated surfaces generally behave weakly catalytic in a large surface temperature range and there is only a small windward surface temperature variation, catalycity can even be modeled with sufficient accuracy by constant overall recombination coefficients.

The catalytic behavior of C/SiC and SiC-surfaces investigated here changes from weakly to strongly catalytic in a large surface temperature range.[13] Furthermore, for high surface temperature nose and body-flap regions the surface temperature can change significantly and hence also the catalytic behavior. Therefore, the non-Arrhenius behavior of recombination coefficients and overall recombination coefficients have to be taken into account by detailed and global catalysis models, respectively.

Validation

The validation of the enhanced code is performed against various free-flight experiments. These experiments have been partially recomputed to demonstrate the influence of the enhancements. The influence of the enhanced modeling on postshock, boundary layer and wake flow and the aerothermal loads is discussed in detail for low to high reentry velocities. To demonstrate the improved modeling and credibility of the enhanced URANUS code, measured aerothermal loads are reconstructed along flight trajectories in a wide gas state and velocity range.

Sharma/Gilmore Air Nozzle Flow

The Sharma/Gilmore air nozzle flow experiment[14] is reconstructed to validate the enhanced URANUS code for an expanding airflow.[8] Total temperature and pressure are 2500 K and 85.7 bar, respectively. Nozzle geometry and Mach-number contours are shown in Fig. 1a. Because of the low translational temperature, no significant chemical reactions occur. The temperature distributions along the nozzle centerline are shown in Fig. 1b. Measured rotational temperature T_r and vibrational temperatures are accurate within ± 100 and ± 75 K, respectively. $T_r = T$ (where T-translational temperature) was computed by the URANUS code.

The measured rotational temperature T_r and the vibrational temperatures of nitrogen $T_{v,N2}$ and oxygen $T_{v,O2}$ can be reconstructed with good agreement. As shown in Fig. 1b, the V-V exchange significantly influences the relaxation process, whereas the C-V exchange (not shown) is almost negligible. The V-V transition probabilities of Rapp were used to compute the V-V energy exchange for the low translational temperatures. Hence, this experiment is particularly well suited to validate the V-V exchange model in the low temperature range.

FIRE II

In 1964 the FIRE reentry experiment was performed in the frame of the Apollo moon program. During Earth reentry, total and radiative heat fluxes at the surface were measured. Nose radius and

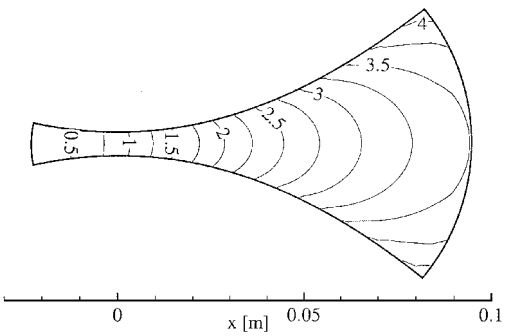

a) Nozzle geometry, Mach-number contours

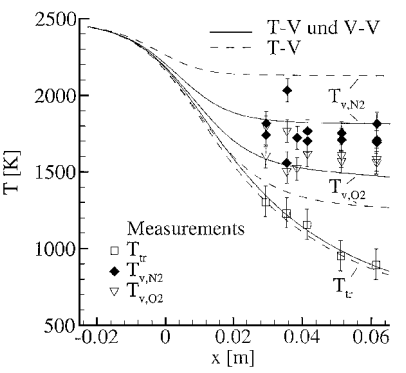

b) Nozzle axis temperature distributions

Fig. 1 Sharma/Gilmore air nozzle flow.

shoulder diameter of the capsule are 0.935 and 0.672 m, respectively. No ablation is considered in the computations. Instead, a radiation equilibrium fully catalytic surface is assumed.

At an altitude of 67 km, the velocity was 11.25 km/s. The computed radiative heat flux is about 15% of the total heat flux.[8] This high velocity flow is completely dissociated and significantly ionized (ionization degree of 10%) with significant thermal nonequilibrium in the postshock region and a region of thermal and chemical equilibrium between the shock and the edge of the boundary layer (Figs. 2b and 2c). We investigated whether the newly implemented electronic excitation influences the ionization rate of atoms for this significantly ionized flow.[7]

As shown in Fig. 2a, the QSS theory predicts a weak subpopulation in the postshock region and an overpopulation in the boundary layer. Even though the subpopulation is weak in the postshock region, the global ionization rate, which is strongly dependent on the population of the upper energy levels, is significantly influenced. As can be seen in Fig. 2b, the global ionization rate computed from the QSS theory is significantly smaller compared to the rate computed from the Boltzmann distribution. Therefore, ionization is significantly delayed by the electronic excitation in the postshock region, as can also be seen from the stagnation line mole fraction distribution of atomic ions N^+ and O^+ in Fig. 2c.

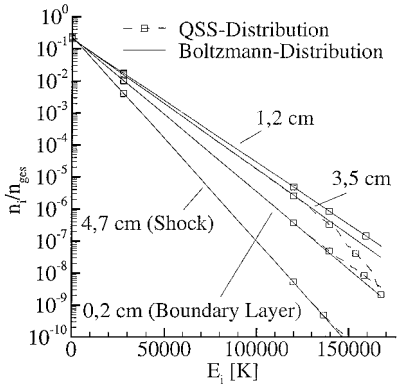

a) Population of electron energy levels

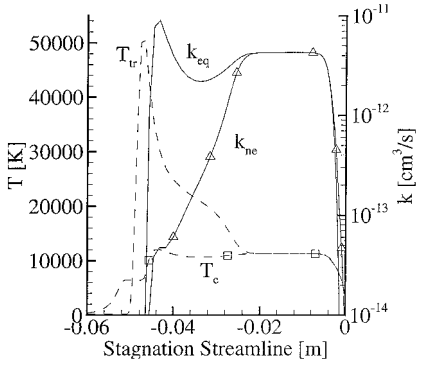

b) Global-rate coefficients, translational and electron temperatures

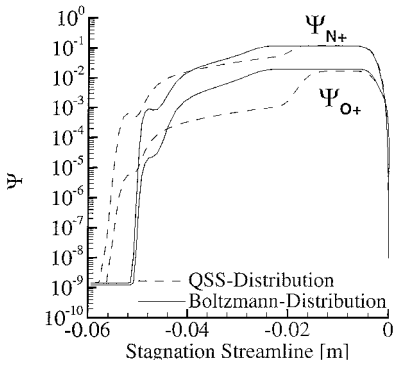

c) Mole fractions of atomic ions N^+ and O^+

Fig. 2 FIRE II: Influence of the electronic excitation on the ionization of N and O.

STARDUST

STARDUST will be the first mission to return samples from beyond the Earth-Moon system. The comet sample return capsule will reenter Earth's atmosphere in 2006. Preflight nose and shoulder diameters of the capsule are 0.44 and 0.812 m, respectively.

The influence of mixing rules on postshock relaxation and surface heat flux was investigated for the partially ionized flow around the STARDUST capsule at an altitude of 84 km and a velocity of 13 km/s. The ionization degree was about 1%. Ablation was not taken into account in the URANUS simulations. Instead, a radiation equilibrium fully catalytic surface was assumed. Because of the small nose radius, the radiative heat flux was neglected.

Using Capitelli's newly computed collision integrals, the mixing rule of Chapman–Cowling (C–C) was compared to the mixing rule of Gupta and Yos.[11] Figure 3a shows the temperature distributions along the stagnation streamline. Because of a more physical model of the ambipolar diffusion, the upstream diffusion of electrons is more physical for the C–C model. As can be seen in Fig. 3b, the more accurate model for the transport processes leads to larger mole fractions of N^+ and O^+ in the postshock region. In the very hot nonequilibrium boundary layer (Fig. 3a) the mixing rules also influence the heat flux to the surface because slight differences between heat conductivities computed with the C–C and Yos/Gupta model arise by mass diffusion caused by oxygen dissociation. The C–C model leads to a 0.9% lower stagnation-point heat flux.

MIRKA Reentry Experiment

MIRKA is a German experimental capsule with a spherical shape of 1 m in diameter and a two-layer TPS that consists of a carbon-phenolic ablator covered by an integral C/SiC heat shield. MIRKA was successfully flown in October 1997.

An objective of the code validation was to investigate whether the heat-flux distribution at a finite rate catalytic surface could be reconstructed with the URANUS code using a simplified global

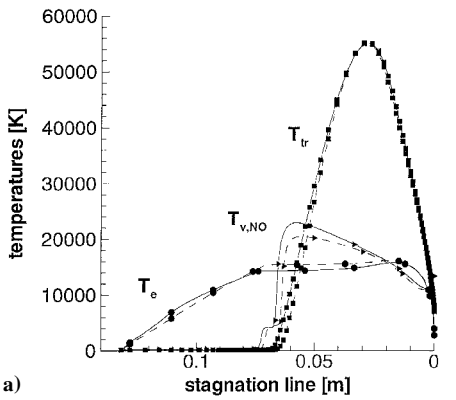

a)

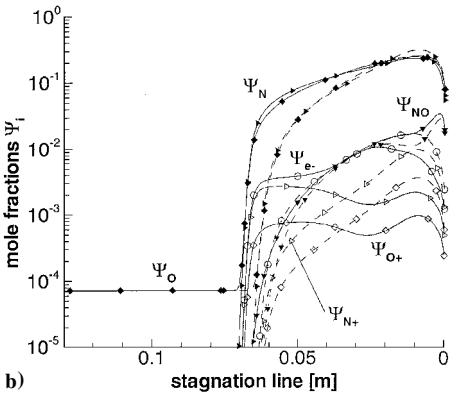

b)

Fig. 3 STARDUST capsule: Influence of the mixing rules on the postshock relaxation (——, Chapman–Cowling approximation, and – – –, Yos/Gupta model).

catalysis model. The MIRKA experiment is well suited for the code validation because of its simple geometry, laminar flow conditions and integral C/SiC heat shield for which measured non-Arrhenius, temperature-dependent overall recombination coefficients are available.

A consistent postflight URANUS code validation has been performed.[15] The postflight trajectory was recomputed from measured acceleration (error within 0.015 g), and stagnation-point pressure. The upstream flow conditions were computed from measured surface conditions and acceleration measurements and therefore do not rely on standard atmosphere data used to compute the design trajectory.

Pressure and temperature were measured along the surface. The surface heat flux has also been reconstructed from temperature measurements inside the heat shield within the HEATIN experiment (thermocouple positioning errors of ±0.3 mm typically lead to surface heat flux errors of 5–10%).

A detailed computation of the aerothermal surface loads has been performed with the URANUS code for several trajectory points.[15] The temperature-dependent catalytic overall recombination coefficients for a SiC surface measured[13] up to 1840 K were used within the phenomenological catalysis model.

Figure 4 shows the time history of surface pressure and heat flux along the design and postflight trajectories. The forebody surface heat-flux distributions for three trajectory points are shown in Fig. 5. Because of the flow expansion around the forebody, the translational temperature drops significantly from the stagnation point to the shoulder of the capsule, and therefore the catalytic behavior changes from weakly catalytic in the stagnation-point region to strongly catalytic in the shoulder region.

As shown in Fig. 5, the measured surface heat-flux distibution can be reconstructed with good agreement along the trajectory with exception of the stagnation region under peak heating conditions. Under the latter conditions the computed stagnation-point temperature is as high as 2063 K. Therefore, surface oxidation reduction reactions occur, which cannot be described with a catalysis model. Presently, a detailed SiC surface reaction model is being developed

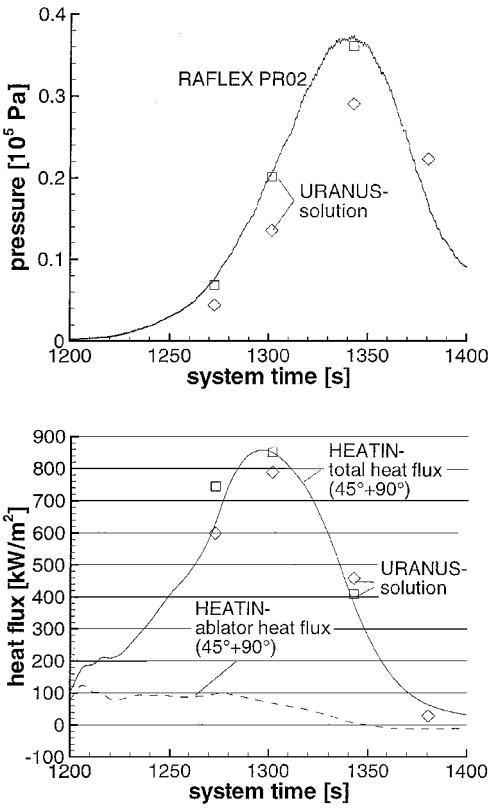

Fig. 4 MIRKA: History of measured and computed surface loads (——, measurements; □, postflight trajectory computations; and ◇, design trajectory computations).

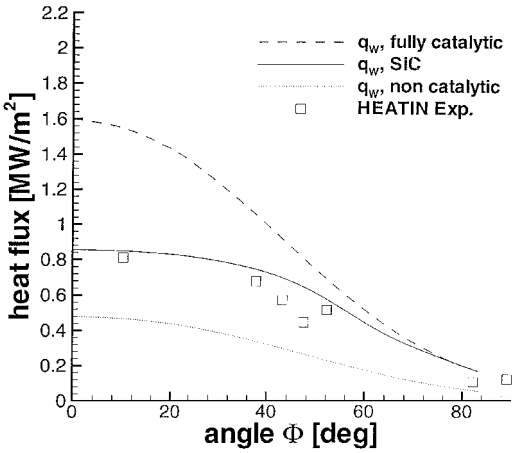

System time 1273 s; freestream velocity, density, pressure: 7372 m · s^{-1}, 1.33 × 10^{-4} kg · m^{-3}, and 8.7 Pa

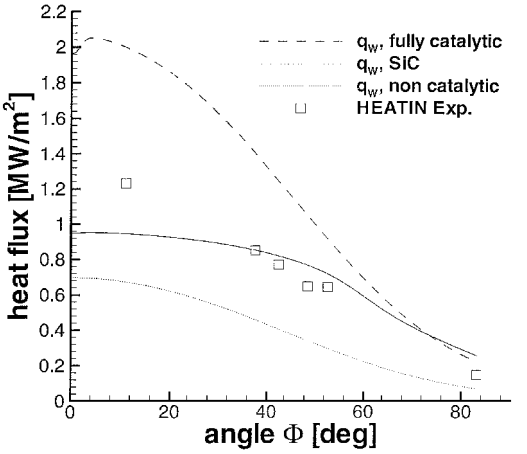

System time 1301; freestream velocity, density, pressure: 6633 m · s^{-1}, 4.91 × 10^{-4} kg · m^{-3}, and 36.8 Pa

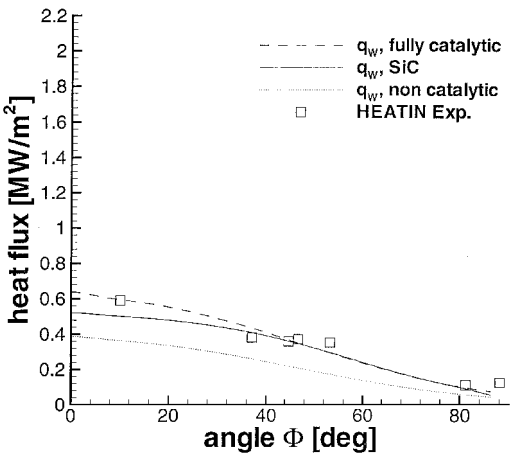

System time 1346 s; freestream velocity, density, pressure: 3652 m · s^{-1}, 2.94 × 10^{-3} kg · m^{-3}, and 220.8 Pa

Fig. 5 MIRKA: Surface heat-flux distributions for three trajectory points.

for these high surface temperature conditions. In the following section we will investigate whether aerothermal loads at nonconvex SiC surfaces can be reconstructed accurately enough under more complex flow conditions.

Body-Flap Experiment

A high-enthalpy hot SiC surface body-flap experiment has been performed in the arc-heated DLR L3K plasma wind tunnel.[16] This experiment can be used to validate the thermochemical gas-phase modeling and the phenomenological catalysis model for a complex,

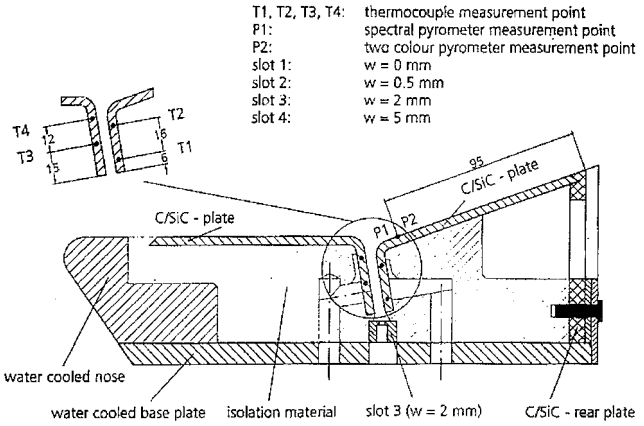

Fig. 6 Body-flap model geometry.

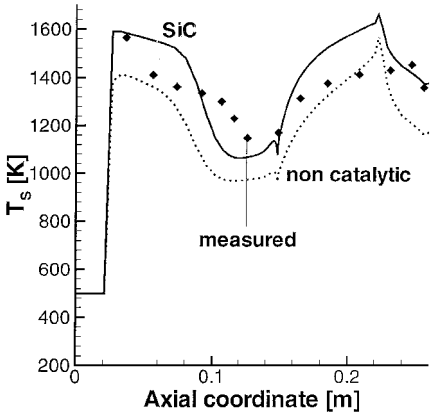

Fig. 7 Predicted and measured body-flap surface temperature distributions.

largely separated, laminar flow along a body-flap model. The geometry of the small model is shown in Fig. 6. The nose of the model is water cooled, and its surface temperature was measured as 500 K. C/SiC plates (4 mm thick), coated with a thin chemical vapor deposition-SiC layer, cover the forebody-flap model. The computations were performed for the model with a closed gap. The model was placed in the plasma jet at an angle of attack of 15 deg. The flap-angle deflection was 20 deg. The reservoir conditions were computed from measured mass flow and total pressure assuming chemical equilibrium. The nozzle flow was computed using a quasi-one-dimensional nonequilibrium code leading to the upstream flow data: total enthalpy 14 MJ/kg, velocity 4160 m/s, density 3.87×10^{-4} kg/m^3.

The SiC-surface catalycity is again computed with the overall recombination coefficients measured by Stewart.[13] Furthermore, radiation equilibrium is assumed at the surface without considering nonconvex radiation effects. The surface total emissivity was 0.87.

The test time was 240 s, and surface temperature was measured with an infrared-camera with a measurement range of 623–2273 K. Very good repeatability of surface temperature measurements was reported.[16] Predicted and measured surface body-flap temperature distributions are shown in Fig. 7. As can be seen, surface temperature distributions computed for noncatalytic and finite rate catalytic surface behaviors disagree to a large extent. In addition, the measured surface temperature distribution is different form the computed results. This is probably because of significant longitudinal heat fluxes in the 4-mm-thick plates that arise because of the very large streamwise surface temperature gradients along the small model. An important phenomenon in the body-flap flow is the very large streamwise variation of the catalytic behavior from weakly catalytic to strongly catalytic, as shown in Fig. 8, and the associated streamwise transport of atomic nitrogen and oxygen in the boundary layer, which strongly influences the surface temperature distribution.

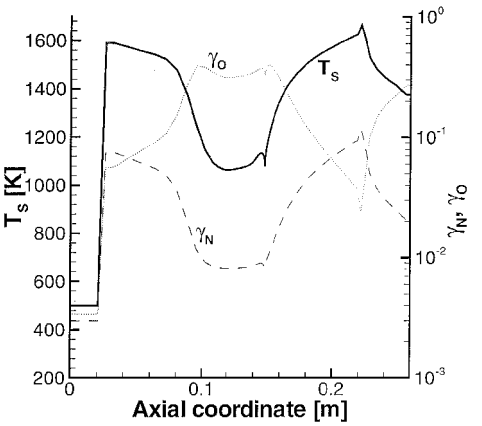

Fig. 8 Overall recombination coefficients and surface temperature distribution along the body-flap surface.

This catalytic variation explains the streamwise surface temperature shift between the noncatalytic and the finite rate catalytic computation in Fig. 7. To reconstruct the measured surface temperature distribution, it seems necessary to account for the thermal flow-structure interaction. Recently the finite rate catalytic surface temperature distribution was computed along the windward side of the X-38 vehicle. Similar finite rate catalycity effects were found along the SiC-coated body flap.[17]

Conclusion

With the enhanced URANUS code high-enthalpy flows can be computed that account for translational, vibrational, rotational, and electronic energies. The transport coefficient modeling is enhanced by Capitelli's new collision integrals and by the more accurate mixing rule of Chapman–Cowling. In addition global and detailed catalysis models for SiO_2 and SiC surfaces have been incorporated.

Rotational excitation leads to higher dissociated flows and to significant $T - T_r$ nonequilibrium under rarefied conditions, and electronic excitation delays the postshock ionization of atoms in partially ionized flows. The enhanced transport coefficient modeling allowed a more accurate prediction of the thermochemical relaxation in the shock region of partially ionized flows.

Finite rate catalysis strongly influences the surface heat flux in nonequilibrium boundary layers and seems to be accounted for accurately enough with global or detailed models.

Aerothermal forebody surface loads of the MIRKA capsule were numerically reconstructed along the postflight trajectory with good agreement. The surface temperature distribution of the body-flap experiment was significantly determined by the large streamwise variation of the catalytic behavior. Finite rate catalytic flap temperatures can exceed those computed with the fully catalytic design assumption.

Acknowledgments

The authors would like to thank the Deutsche Forschungsgemeinschaft and the ESA for their support.

References

[1]Frühauf, H.-H., Fertig, M., Olawsky, F., and Bönisch, T., "Upwind Relaxation Algorithm for Reentry Nonequilibrium Flows," *High Performance Computing in Science and Engineering 99*, Springer–Verlag, Berlin, 2000.

[2]Knab, O., Frühauf, H.-H., and Messerschmid, E., "Theory and Validation of the Physically Consistent Coupled Vibration-Chemistry-Vibration Model," *Journal of Thermophysics and Heat Transfer*, Vol. 9, No. 2, 1995, pp. 219–226.

[3]Kanne, S., Knab, O., Frühauf, H.-H., and Messerschmid, E.W., "The Influence of Rotational Excitation on Vibration-Chemistry-Vibration-Coupling," AIAA Paper 96-1802, June 1996.

[4]Kanne, S., Knab, O., Frühauf, H.-H., Pogosbekyan, M., and Losev, S. A., "Calibration of the CVCV-Model Against Quasiclassical Trajectory Calculations," AIAA Paper 97-2557, June 1997.

[5]Kanne, S., Gogel, T. H., Dupuis, M., Messerschmid, E. W., and Roberts, T. P., "Simulation of Radiation Experiments on Reentry Vehicles Using the New Radiation Database PARADE," AIAA Paper 97-2562, 1997.

[6]Gogel, T. H., "Numerische Modellierung von Hochenthalpieströmungen mit Strahlungsverlusten," Ph.D. Dissertation, Fakultüt für Luft- und Raumfahttechnik, Univ. Stuttgart, Stuttgart, Germany, 1994.

[7]Kanne, S., "Thermochemical Relaxations Through Collisions and Radiation," *Journal of Thermophysics and Heat Transfer* (submitted for publication).

[8]Kanne, S., "Zur Thermo-Chemischen Relaxation Innerer Freiheitsgrade durch Stoß- und Strahlungsprozesse beim Wiedereintritt," Ph.D. Dissertation, Fakultät für Luft- und Raumfahrttechnik, Univ. Stuttgart, Stuttgart, Germany, 2000.

[9]Rapp, D., "Interchange of Vibrational Energy Between Molecules in Collisions," *Journal of Chemical Physics*, Vol. 43, No. 1, 1965, pp. 316, 317.

[10]Park, C., *Nonequilibrium Hypersonic Aerothermodynamics*, Wiley, New York, 1990.

[11]Fertig, M., Dohr, A., and Frühauf, H.-H., "Transport Coefficients for High-Temperature Nonequilibrium Air Flows," AIAA Paper 98-2937, June 1998; *Journal of Thermophysics and Heat Transfer* (to be published).

[12]Daiss, A., Frühauf, H.-H., and Messerschmid, E. W., "Modeling of Catalytic Reactions on Silica Surfaces with Consideration of Slip Effects," *Journal of Thermophysics and Heat Transfer*, Vol. 11, No. 3, 1997, pp. 346–352.

[13]Stewart, D., "Determination of Surface Catalytic Efficiency for Thermal Protection Materials—Room Temperature to Their Upper Use Limit," AIAA Paper 96-1863, June 1996.

[14]Gilmore, J. O., Sharma, S., Bose, D., and Candler, G., "On Kinetics Modeling of Vibrational Energy Exchange with Application to the Nozzle Flow Problem," AIAA Paper 97-0134, Jan. 1997.

[15]Fertig, M., and Frühauf, H.-H., "Detailed Computation of the Aerothermodynamic Loads of the MIRKA Capsule," *Proceedings of the 3rd European Symoposium on Aerothermodynamics for Space Vehicles*, ESTEC, Noordwijk, The Netherlands, 1998, pp. 703–710.

[16]Gülhan, A., "Investigation of Gap Heating on a Flap Model in the Arc Heated Facility L3K," DLR, Rept. TET-DLR-21-TN-3101, 1999.

[17]Fertig, M., and Frühauf, H.-H., "Reliable Prediction of Aerothermal Loads at TPS-Surfaces of Reusable Space Vehicles," 12th European Aerospace Conf., Nov.–Dec. 1999.

M. Torres
Associate Editor